catalysts

MDPI

Article

Effectively Synthesizing SO_4/TiO_2 Catalyst and Its Performance for Converting Ethanol into Diethyl Ether (DEE)

Karna Wijaya [1,*], Alya Rahmadhani Putri [1], Sri Sudiono [1], Sri Mulijani [2], Aep Patah [3], Arief Cahyo Wibowo [4] and Wahyu Dita Saputri [5]

1 Department of Chemistry, Faculty of Mathematics and Natural Sciences, Universitas Gadjah Mada, Yogyakarta 55281, Indonesia; alyarahmadhani@mail.ugm.ac.id (A.R.P.); ssudiono@ugm.ac.id (S.S.)
2 Department of Chemistry, Faculty of Mathematics and Natural Sciences, Institut Pertanian Bogor, Bogor 16680, Indonesia; srimulijani@apps.ipb.ac.id
3 Department of Chemistry, Faculty of Mathematics and Natural Sciences, Institut Teknologi Bandung, Bandung 40116, Indonesia; aep@chem.itb.ac.id
4 Department of Applied Sciences, College of Arts and Sciences, Abu Dhabi University, Abu Dhabi 59911, United Arab Emirates; arief.wibowo@adu.ac.ae
5 Research Center for Physics, National Research and Innovation Agency (BRIN), South Tangerang 15314, Indonesia; wahy050@brin.go.id
* Correspondence: karnawijaya@ugm.ac.id

Abstract: This SO_4/TiO_2 catalyst as a heterogeneous acidic catalyst was synthesized in various concentrations of H_2SO_4. The activity and selectivity of the SO_4/TiO_2 catalyst on the dehydration reaction of ethanol to diethyl ether were studied as well. The SO_4/TiO_2 was prepared from TiO_2 powder by wet impregnation method with a various aqueous solution of H_2SO_4 (1; 2; 3 M H_2SO_4) and calcination temperature (400, 500, and 600 °C) to obtain a catalyst with optimum acidity. The catalysts were characterized using FTIR, XRD, SEM-EDX, SAA, TGA/DSC, and acidity test gravimetrically with ammonia. The liquid product of DEE was analyzed by gas chromatography (GC) to analyze the selectivity of the catalyst. The catalyst TS-3-400 had the highest activity and selectivity in the dehydration reaction of ethanol to diethyl ether at a temperature of 225 °C, with a conversion of 51.83% and a DEE selectivity of 1.72%.

Keywords: diethyl ether; ethanol dehydration; sulfated titania

check for updates

Citation: Wijaya, K.; Putri, A.R.; Sudiono, S.; Mulijani, S.; Patah, A.; Wibowo, A.C.; Saputri, W.D. Effectively Synthesizing SO_4/TiO_2 Catalyst and Its Performance for Converting Ethanol into Diethyl Ether (DEE). *Catalysts* **2021**, *11*, 1492. https://doi.org/10.3390/catal11121492

Academic Editors: Francesca Raganati and Alessandra Procentese

Received: 18 November 2021
Accepted: 1 December 2021
Published: 6 December 2021

Publisher's Note: MDPI stays neutral with regard to jurisdictional claims in published maps and institutional affiliations.

Copyright: © 2021 by the authors. Licensee MDPI, Basel, Switzerland. This article is an open access article distributed under the terms and conditions of the Creative Commons Attribution (CC BY) license (https://creativecommons.org/licenses/by/4.0/).

1. Introduction

The expected gradual depletion of fossil fuels and the environmental impacts from the fuel exhaust gas has drawn attention to establishing renewable energy sources. Ethanol, derived from biomass, has stood out as a source of clean and renewable biofuel. In addition, there is a growing interest in using ethanol in biorefineries to synthesize larger molecules. Ethanol is a green alternative to petroleum in the production of olefins and aromatics, and it can also be employed in the production of several oxygenated molecules, such as 1-butanol, acetaldehyde, and diethyl acetate [1–3].

Production of petrochemicals from a non-petroleum, environmentally feedstock and development of new, efficient ethylene production processes are considered as challenging research areas [4,5]. At present, the development of alternative energy is commonly performed to restrict those issues. The use of alternative renewable fuels for diesel engines has been endorsed worldwide because of fossil gas depletion and the damaging effect of petroleum gas combustion on the environment [6]. One alternative energy that may be used is renewable bioethanol [7].

Biodiesel is one of the most promising renewable fuels used for diesel engines without engine modification [8]. Among the oxygenated options, dimethyl ether (DME) and diethyl ether (DEE) appeared as one of the promising fuels or an oxygen additive for diesel engines with its benefits of an excessive cetane quantity and oxygen content [9]. The production

of DEE is of great interest because, in addition to being an important product in the fine chemicals industry, it is used as a solvent substitute for aromatic solvents and has a number of applications in the fuel chemical industry [10].

The use of ethanol requires a high concentration to become fuel, which is a process that involves much energy. A high-energy separation process is needed to obtain high concentrations of ethanol. This is due to the nature of ethanol and water that forms an azeotropic solution at atmospheric pressure and temperature of 78 °C and 95% [11]. To minimize this energy, the low concentrations of ethanol can be used to convert into DEE products. With limited water solubility and high solubility in oils, fats, and resins, DEE is often used in liquid-liquid extraction processes using the Barbet process [12]. The disadvantage of this method is that catalytic separation is difficult, expensive, and corrosive. The use of a heterogeneous catalyst may accelerate the formation of DEE.

In general, product yields essentially depend on the nature of acid catalyst types used [13,14]. Many solid acid catalysts have been used for dehydration of ethanol, such as metal oxides, zeolites, supported phosphoric acid, alumina, silica-alumina, and heteropoly-acid catalysts. The catalytic activity for ethanol dehydration could be correlated to the number of strong Brønsted acid sites in the catalyst [15–18]. Several studies involving solid acid catalysts such as TiO_2, ZrO_2, Al_2O_3, and H-ZSM-5 for the dehydration of ethanol to diethyl ether have been conducted and gave various yield percentages. Different transition metal oxide catalysts [19,20] were tested for the catalytic dehydration of ethanol.

Titanium dioxide (TiO_2), commonly known as titania, can be used as an acid and base catalyst based on its amphoteric properties. TiO_2 can be used as a heterogeneous catalyst because it is a type of metal oxide catalyst with a high surface area, good chemical stability, and has acid-base properties [21]. The utilization of TiO_2 catalyst as a heterogeneous acid catalyst has been widely studied in SO_4/TiO_2, which shows good catalytic activity. Sulfur treatment with the addition of sulphuric acid will increase the reactivity and acid strength of the catalyst material [22]. This catalyst is also called a solid superacid catalyst which is widely used in the petrochemical industry and oil refining process, which shows better performance compared to other metal sulfate oxides [23].

Several studies that show the success of making SO_4/TiO_2 as a catalyst include research conducted by [24] on the esterification of fatty acids. Other studies have also been conducted by [25], who synthesized SO_4/TiO_2 catalyst through the sol-gel method used in the liquid-phase dehydration of sorbitol to isosorbide, and its selectivity of conversion had been 100% and 75%. The dehydration of ethanol to DEE reaction still receive less attention [15,26]. Considering the importance of ethanol dehydration to DEE and the fact that the role the catalyst should play in determining high selectivity towards DEE is not yet well established, the present work is focused on the dehydration of ethanol over SO_4/TiO_2 catalyst and its influence on the selectivity for DEE.

2. Methods

2.1. Materials

Materials used in this research were nano TiO_2 (titanium dioxide) commercial, Aquadest, and chemicals for analysis from Merck, namely sulfuric acid (H_2SO_4; 98%), ammonia (NH_3), ethanol (C_2H_5OH; 96%), and N_2 gas.

2.2. Preparation of Catalysts

Preparation of SO_4/TiO_2 catalysts were carried out by the wet impregnation method. Ten g of TiO_2 was mixed with 150 mL of H_2SO_4 solution (1; 2; 3 M), and the mixture was stirred for 24 h using a magnetic stirrer. The mixtures were then centrifuged for 20 min with the speed of 2000 rpm to separate the solids from the mixture. The solid obtained were dried in the oven at 105 °C overnight and were denoted as TS-1, TS-2, and TS-3. The products were then characterized using FTIR and NH_3 adsorption. The products were then ground and sieved using a 200 mesh sieve. Material with the highest acidity was calcined

in various temperatures at 400, 500, 600 °C for 4 h. Material with the highest acidity was denoted as TS-3-400, TS-3-500, and TS-3-600 then the acidity of materials was tested.

2.3. Characterization of Catalysts

Catalysts were characterized using *Fourier Transform Infrared* (FTIR) series Nicolet Avatar 360 IR to study functional groups in the samples. Catalysts characterized using *X-ray Diffraction* (XRD) series Shimadzu Model XRD 6000 used to know the crystallinity of catalyst. Characterization using TGA/DTA (*Thermogravimetric Analysis-Differential Scanning Calorimetry*) was done to study thermal properties and phase changes due to enthalpy changes of material. Characterization using SEM-EDX model Phenom Desktop ProXL was performed to determine the surface condition and composition of elements in the sample. Characterization using Surface Area Analyzer (SAA) was done to measure the surface area and pore size of the sample.

The acidity test of catalysts was conducted with a gravimetry method using ammonia vapour as an adsorbate base. Empty porcelains were prepared and heated at 100 °C for 2 h, and then porcelains were weighed as W_0. A total of 0.05 g of samples TS0, TS-1, TS-2, and TS-3 were put in porcelains and heated at 100 °C for 2 h and weighed as W_1. Porcelains containing catalysts were inserted into the desiccator in a closed state. Furthermore, ammonia vapour was flown towards the desiccator for 30 min. Samples were put for 24 h and after were weighed as W_2. The total acidity value was determined using the formula:

$$\text{Acidity} = \frac{W_2 - W_1}{(W_1 - W_0) \times \text{MW NH}_3} \times 1000 \text{ mmol g}^{-1}$$

where:

W_0: weight of empty porcelains (g)
W_1: weight of crucible porcelain + sample before adsorption (g)
W_2: weight of crucible porcelain + sample after adsorption (g)
MW NH_3: molecular weight of NH_3 (mol g^{-1})

2.4. Application of Catalyst

In this research, TS0 and TS-3-400 catalysts were applied to the dehydration process to convert ethanol into DEE. The dehydration process was carried out in a reactor with an N_2 gas flow rate of 20 mL/min at various temperatures of 175, 200, and 225 °C using 1 g of catalyst and 10 mL of ethanol. Products from results of dehydration process were determined percentage (%) conversion of its liquid products using the following calculation:

$$\text{Liquid product conversion} = \frac{m_{\text{ethanol(in)}} - m_{\text{ethanol(out)}}}{m_{\text{ethanol(out)}}} \times 100\%$$

$$\text{Yield DEE} = \frac{E_i}{E_{\text{total}}} \times 100\%$$

where:

m_{ethanol}: mass of ethanol (g)
E_i: peak area of DEE in GC chromatogram
E_{total}: total peak area in GC chromatogram

3. Results

3.1. Characterization of Catalyst

3.1.1. FTIR and Acidity Test

Figure 1 shows the FTIR spectra of TS0, TS1, TS2, and TS3. The typical absorption bands that appeared in the FTIR spectra of TiO_2 and SO_4/TiO_2 with various concentrations were the sharp absorption bands at 3402–3441 cm^{-1}, which were the stretching vibrations of-OH and at 1630 cm^{-1}, which was the bending vibrations of-OH from H_2O coordinated

with the material [24]. The occurrence of the bending and stretching vibrations of -OH from H_2O was due to the presence of water vapour in pure TiO_2 and sulfate TiO_2. The intensity of the absorption peak increased with increasing of SO_4^{2-} concentration due to the number of hydrogen bonds in the catalyst. The results of the TiO_2 and SO_4/TiO_2 sample spectra showed the same absorption peak in the 400–850 cm^{-1} region, which represented the vibration of the stretching of the O-Ti-O bond [27] where the peaks were 400–510 and 550–615 cm^{-1} were the stretching vibration of Ti-O [28].

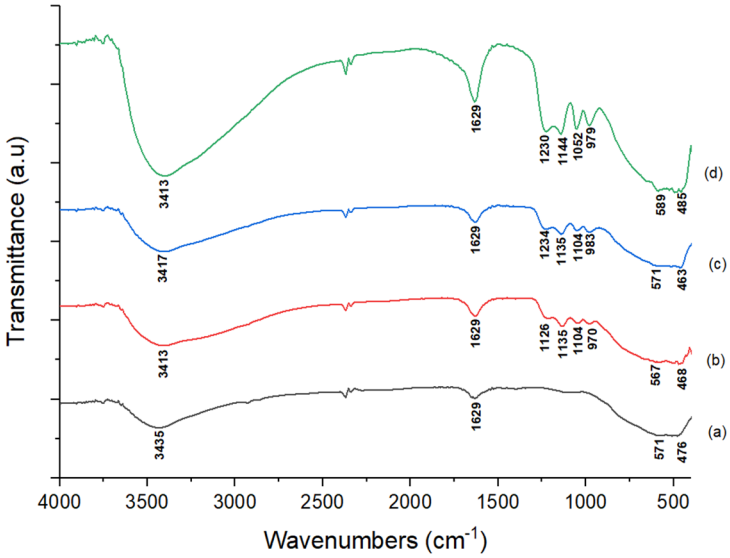

Figure 1. FTIR spectra of (a) TS0, (b) TS1, (c) TS2, and (d) TS3.

The FTIR spectra of SO_4/TiO_2 in the variation of concentrations had four new bands appeared at the region of 979–1226 cm^{-1}. The four bands were asymmetrical vibration of S=O, symmetry vibration of S=O, asymmetric vibration of S-O, and symmetry vibration of S-O which appeared at 1226, 1134, 1049, and 979 nm^{-1}, respectively [29]. The results showed the presence of sulfate ion bonded with titania cations. From these spectra, it could be seen that the occurrence of S-O and S=O vibrations confirmed the presence of sulfate ions bonded to the surface of the titania [24]. Based on the FTIR spectra shown in Figure 1, it was illustrated that the intensity of the sulfate ion absorption band had increased along with the increasing concentration of the sulfuric acid used in the sulfation process. The higher the SO_4^{2-} concentration, the more sulfate ions bonded to the surface of the titania. The highest SO_4^{2-} absorption peak intensity was demonstrated by the catalyst TS-3 which also suggested that the catalyst TS-3 had a high acidity value. FTIR spectra could only show data qualitatively, so an acidity test was needed to quantitatively determine the total acidity possessed by SO_4/TiO_2 catalysts at various concentrations using the gravimetric method. The acidity test of the catalyst to determine the number of acid sites present on the catalyst was carried out by the gravimetric method using NH_3 solution in a vacuum. Table 1 shows the total acidity value of catalysts.

Table 1. Acidity test of catalysts.

Catalysts	Total Acidity (mmol g^{-1})
TS-0	8.42
TS-1	12.50
TS-2	14.67
TS-3	17.94

The results of the acidity test showed that the catalyst TiO_2 had an acidity number of 8.42 mmol g^{-1}. The sulfation process affected the acidity of TiO_2. With a higher concentration of sulfate ions, the acidity of the SO_4/TiO_2 catalyst increased due to a large number of

sulfate ions bonded to the surface of the titanium dioxide, which then formed the acidic site of Brønsted as the acid center of the catalyst. The catalyst of TS-3 showed the highest acidity number of 17.94 mmol g $^{-1}$. The catalyst with the highest total acidity content, TS-3 in this research, was run through a calcination process at temperature variations of 400, 500, and 600 °C. This process aimed to determine the effect of temperature on the acid content of the catalyst and determine the optimum temperature based on the highest acidity value in the TS-3 catalyst synthesis process. [27] reported that as the calcination temperature increased, the absorption intensity in the area decreased significantly, indicating that the number of -OH absorbed in the catalyst material decreases as the temperature increased. Table 2 represents the data of total acidity of catalysts after calcination.

Table 2. Acidity test of TS-3 at 400, 500, and 600 °C.

Catalyst	Total Acidity (mmol g^{-1})
TS-3-400	11.35
TS-3-500	6.19
TS-3-600	3.3

Figure 2 shows that the differences in the temperature of calcination affected the strength of the presence of the sulfate ion. There were four absorption bands of sulfate ions at temperatures 400 °C in the wavenumbers of 1230–900 cm^{-1}, while the absorption strength of the sulfate ions began to decrease at temperatures of 500 and 600 °C. At the wavenumbers of 3417 and 1635 cm^{-1} (H_2O vibration), the absorption bands were reduced in the intensity level. This indicated that the water vapor in the TS-3-400 catalyst had decreased to decrease the rate of absorption due to the heating process. As the calcination temperature increased, the absorption intensity in the area decreased significantly, which indicated that the number of -OH had been absorbed into the catalyst material with increasing of temperature [27]. FTIR spectra of TS-3-400 catalyst also showed the appearance of a new specific absorption in the region of the wavenumber 1238 cm^{-1} which was a vibration of symmetry of the S=O bond of SO_4^{2-} ions [29], so that at a higher temperature the absorption in this area was lost, since the S=O bond began to decompose at a calcination temperature of more than 400 °C. The symmetrical vibration of the SO_4^{2-} ion S-O bond in the range of 973–1102 cm^{-1} region also showed the highest intensity at a temperature of 400 °C, which indicated the number of SO_4^{2-} ions that adhered to the TiO_2 surface at this temperature.

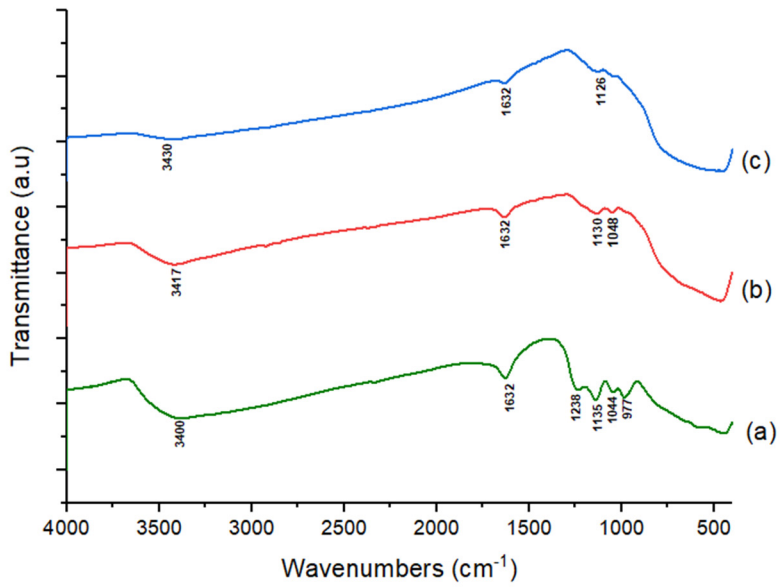

Figure 2. FTIR spectra of (a) TS-3-400, (b) TS-3-500, (c) TS-3-600.

3.1.2. Characterization Using XRD

Figure 3 shows the composition of the crystalline structure of the catalyst indicated at 2θ = 5–90°. [30] found that at temperatures between 550 and 750 °C, the calcined TiO_2 powder only formed the anatase phase. [31] synthesized SO_4/TiO_2 catalyst at 400 °C and discovered the formation of a pure anatase crystallinity process without the formation of rutile or brookite. It was found that sulfate ions were anchored to anatase phases of titania crystals at annealing temperatures of 400–600 °C, since these materials had short O-O atomic bond length, which was larger than the longest O-O bond length of sulfate ions.

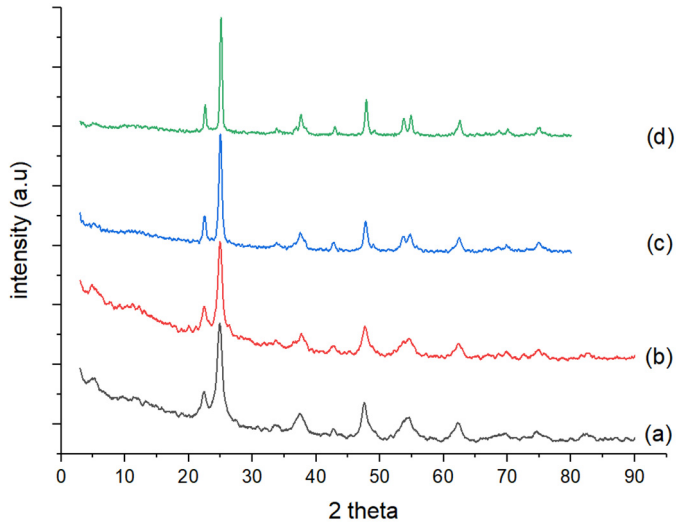

Figure 3. Diffractogram of (a) TS0, (b) TS-3-400, (c) TS-3-500, and (d) TS-3-600.

Therefore, the sulfate ions tended to deform less and were consequently more stable [32]. At a temperature of 800 °C, a mixture of anatase and rutile phases began to form, and at 1000 °C, 100% of the rutile phase was formed [33]. The sulfation process on the surface of TiO_2 caused a decrease in the intensity of the main diffraction peaks of TiO_2. Due to the high concentration of H_2SO_4, TiO_2 dissolved in H_2SO_4, and the amount of SO_4^{2-} ions covering the TiO_2 surface increased, which induced the formation of Ti-O-S, whereby the phase became more amorphous, or the crystallinity decreased [34]. The calcination temperature also affected the crystallinity of the catalyst. The diffractogram of TS-3-400 °C catalyst showed lower crystallinity which was indicated by the lower intensity of the diffraction peaks due to the incomplete calcination process and the number of SO_4^{2-} ions on the surface of TiO_2 that could decrease its crystallinity. Increasing the calcination temperature increased the intensity of the diffraction peak due to decomposition of the SO_4^{2-} ions on the TiO_2 surface so that the crystallinity increased. Furthermore, catalytic calcination at higher temperatures resulted in an increase in catalyst crystal size of 17.25 and 19.73 nm at 500 and 600 °C, respectively. According to [30], increasing calcination temperatures resulted in an increase in crystal size of catalyst SO_4/TiO_2. Table 3 represents the information of crystal size of catalysts.

Table 3. Crystal size of catalysts.

Sample	Crystal Size (nm)
TS0	25.99
TS-3-400	10.03
TS-3-500	17.25
TS-4-600	19.73

3.1.3. Characterization Using SEM-EDX

Figure 4 at a magnification of 5000 times represents the morphology of catalyst TS0 and TS-3-400. The catalyst of TS0 particles has a uniform and darker morphology. Research conducted by [33] suggested that calcination temperature has an effect on changes in TiO_2 particle size. A calcination temperature of 400 °C produced spherical particles with particle size < 20 nm, then at 400 °C it formed larger particles and agglomeration formation occurred and at temperatures of 800 °C and 1000 °C produced particles of non-uniform size due to all agglomeration particles resulting in increased crystalline size.

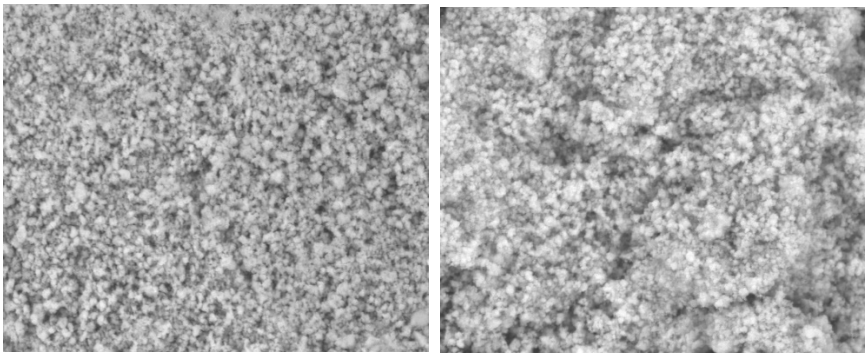

(**a**) (**b**)

Figure 4. SEM image of (**a**) TS0 and (**b**) TS-3-400.

Morphology of catalyst TS0 after sulfation process showed the formation of particles in the form of brighter granules with a slightly larger size due to the formation of agglomeration in the presence of SO_4^{2-} ions bound to TiO_2. The presence of a brighter part of the catalyst surface of TS-3-400 indicates the presence of high-charged ions bound to the catalyst [35]. This explains that the sulfate group has been successfully isolated on the surface of TS0, which was confirmed by the presence of sulfur elements in the catalyst TS-3-400 based on EDX data. Table 4 shows the information of characterization of catalysts TS0 and TS-3-400.

Table 4. Characterization of catalysts TS0 and TS-3-400.

Element	Atom (%)	
	TS0	**TS-3-400**
Ti	28.30	28.26
O	71.70	66.92
S	-	4.82

3.1.4. Characterization Using TGA/DSC

Figure 5 shows thermogram of TS0 and TS-3-400, respectively. The decrease in mass occurred in the temperature range of 50–250 °C, which was associated with the loss of physically adsorbed water molecules. At a temperature of 500–900 °C, a decrease in mass indicated the removal of organic material (polymer chains) in the TiO_2 material and the decomposition of SO_4^{2-} ions adhering to the TiO_2 surface in a TS-3-400. According to [36], the curve of the high mass reduction of the SO_4^{2-} depends on its concentration which was used in the catalyst preparation, the higher the amount or concentration of SO_4^{2-} lead to a mass reduction curve with higher intensity.

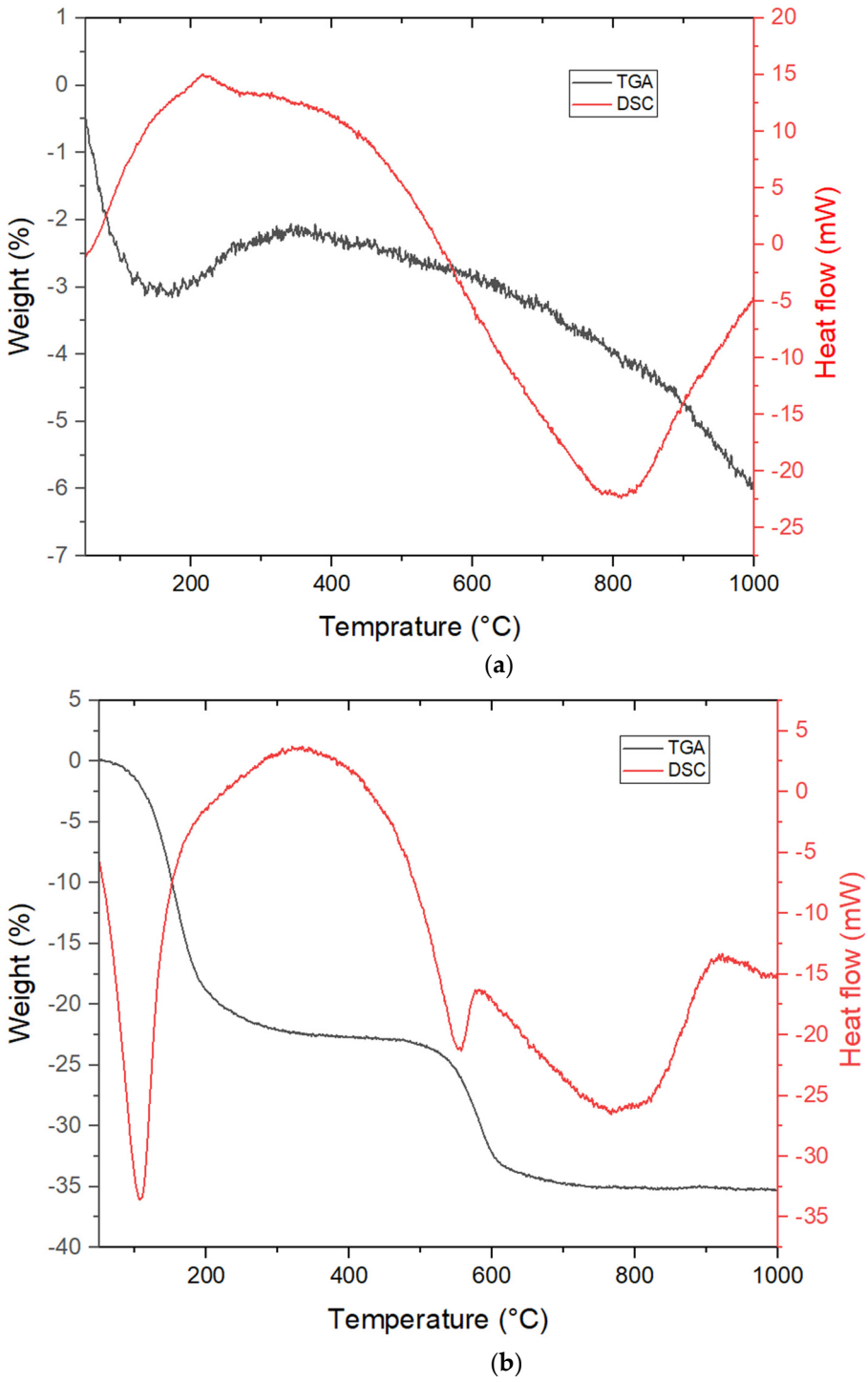

Figure 5. TGA/DSC thermogram of (**a**) TS0 and (**b**) TS-3-400.

The result of the DSC analysis for the TS0 and TS-3-400 catalyst showed the formation of an endothermic curve in the range from 50–150 °C with an enthalpy of 508.6 J/g, which represented the loss of mass of physically adsorbed water molecules on the catalyst material. According to [34], the endothermic curve formed in sulfated titania catalysts in the range of 50–300 °C contributed to the loss of physically adsorbed water and the hydration of the water of the catalyst material. In addition, the endothermic curve in catalyst TS0 in the range of 600–897 °C with an enthalpy of 560.22 J/g indicated the loss of organic material (polymer chains) from the TS0 material, whereas the endothermic curve in the catalyst TS-3–400 in the range 516–573 °C with an enthalpy of 133.56 J/g indicated the

decomposition of the sulfate ion from the solid catalyst TS-3-400 and the formation of the TS0 rutile phase.

3.1.5. Characterization Using SAA

The sulfation process in TS0 material reduced the specific surface area from 94.90 m^2g^{-1} to 9.85 m^2g^{-1}, as well as the total value of the pore volume and the pore diameter of the catalyst by adding sulfuric acid, which covered the surface of the titanium. Table 5 represents the data of textural properties of catalysts TS0 and TS-3-400.

Table 5. Textural properties of catalysts TS0 and TS-3-400.

Catalyst	Surface Area	Total Pore Volume	Pore Diameter
	(m^2g^{-1})	(ccg^{-1})	(nm)
TS0	94.90	0.360	15.17
TS-3-400	9.85	0.073	29.60

The increase in sulfuric acid addition also caused a reduction in the amount of catalyst pores induced by the entry of sulfate groups into the surface of the titanium. The porosity of the material catalyst was caused by the formation of aggregates as a result of the interaction between TiO_2 and SO_4^{2-} ions [36]. Ref. [37] also reported that the specific surface area of TiO_2 had decreased from 80.90 m^2g^{-1} to 48.96 m^2g^{-1} on SO_4/TiO_2. Both samples had the same isotherm curve profile, which was the adsorption–desorption isotherm type IV, which showed a characteristic of mesopore materials with pore diameters of 2–50 nm, i.e., 15.18 nm for TS0 and 29.60 nm for TS-3-400. Figure 6 shows the adsorption-desorption curve of TS0 and TS-3-400.

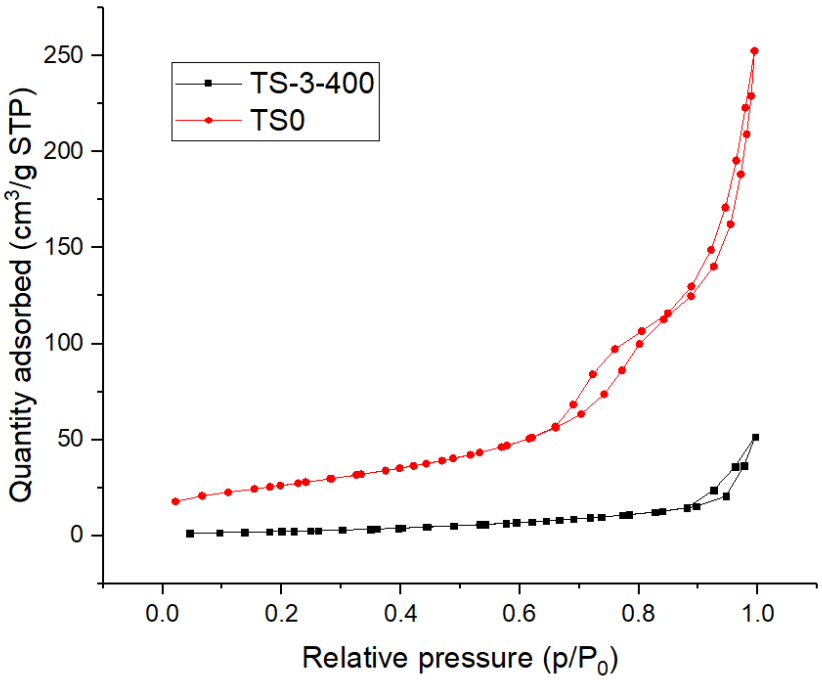

Figure 6. Adsorption-desorption curve of TS0 and TS-3-400.

3.2. Application of Catalyst

3.2.1. Test of Catalysts Activity toward Dehydrated Liquid Products

Catalyst activity tests were carried out to assess the catalysts that were synthesized to convert baits (ethanol) into biofuels (diethyl ether). Dehydration process was carried out at temperatures of 175–225 °C with a gas flow rate of N_2 of 20 mL/min for 60 min.

Figure 7 presents the data of conversion percentage on dehydration reaction using catalysts TS0 and TS-3-400 at various temperatures of 175, 200, and 225 °C. The liquid products conversion using catalyst TS-3-400 at various temperatures was higher compared to catalyst TS0. This was due to the addition of sulfate to titania catalyst increased the number of Brønsted acid and Lewis acid sites in catalysts, where acid strength was the most influential factor in determining catalytic activity in ethanol dehydration reaction [37]. Strong acid sites influenced improved the catalytic activity of the SO_4/TiO_2 catalyst.

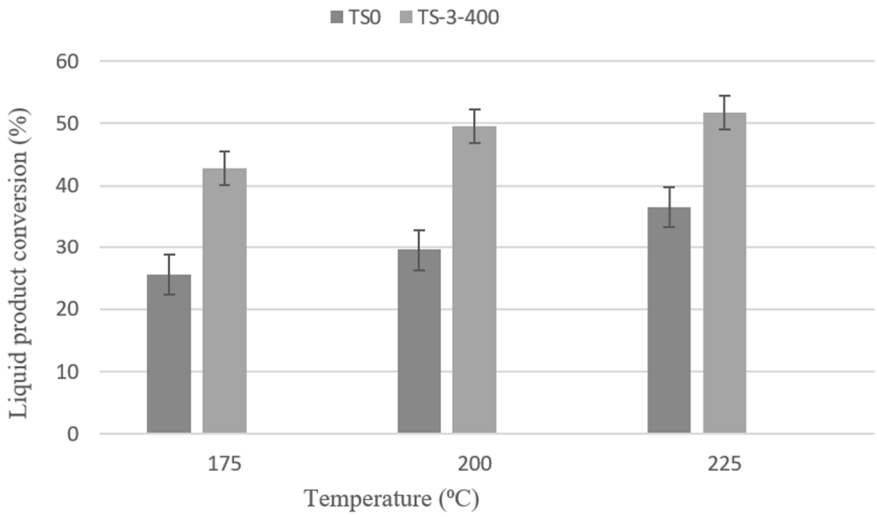

Figure 7. Liquid product conversion of dehydration reaction.

According to [13] the presence of Lewis and Brønsted acid sites number could be determined by NH_3-TPD analysis. It showed that TiO_2 contained several weak acids, and medium acid sites. The addition of SO_4^{2-} ions increases the acidity of TiO_2, which was indicated by the presence of weak acid, medium acid and strong acid sites and the higher the SO_4^{2-} ion concentration showed the more medium acid and strong acid sites. Strong acid sites influenced improved the catalytic activity of the SO_4/TiO_2 catalyst.

3.2.2. Selectivity Test for Dehydrated Liquid Products

The chemical composition of the product and the selectivity of the catalyst were determined using Gas Chromatography (GC) analysis. The ability of a catalyst to convert ethanol into diethyl ether was referred as catalyst selectivity. The percentage of diethyl ether content based on GC analysis data was used to determine selectivity. In this research, catalytic activity was tested using TiO_2 and TS-3-400 in an ethanol dehydration reaction using 3 various temperatures of 175, 200, and 225 °C.

The results of DEE levels in ethanol dehydration reactions with TS-3-400 catalysts were compared to results obtained from TS0 catalyst shown in Figure 8. Diethyl ether levels were 0% in the catalytic reaction using TS0 catalyst at a temperature of 175, 200, and 225 °C. The difference in the results demonstrated that the reaction temperature and treatment of the catalyst were critical in the ethanol dehydration reaction. While DEE levels in the catalyst of TS-3-400 increased as the reaction temperature increased. This indicated that the ideal temperature for ethanol dehydration to diethyl ether was 225 °C with a DEE content of 1.72%. According to the Arrhenius equation, rising temperatures could increase ethanol conversion. From the equation, an increase in temperature would increase the constant reaction speed, thereby increasing the reaction rate [38].

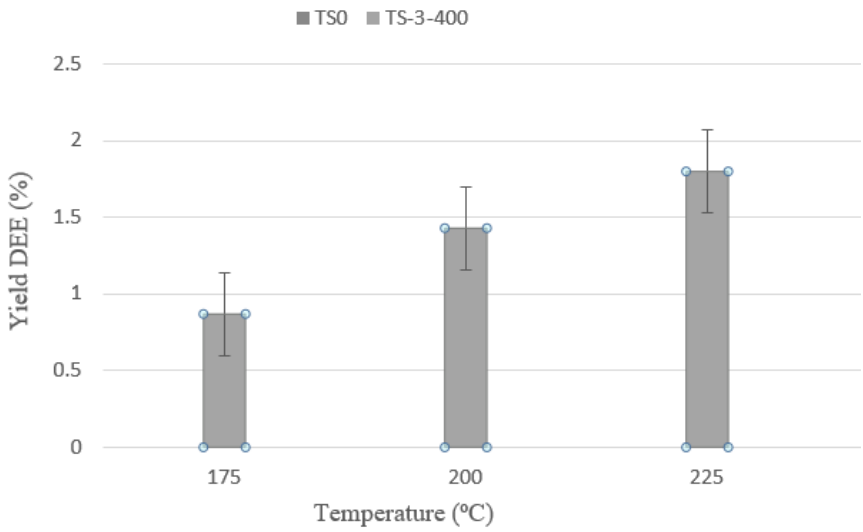

Figure 8. Yield DEE in various temperature of dehydration reaction.

The result of dehydration reaction of ethanol to diethyl ether using a heterogeneous catalyst SO_4/TiO_2 was still low. Research conducted by [39] showed that the alumina catalyst used in the dehydration process of ethanol to diethyl ether produced more diethyl ether of 2.41%. However, when compared to the heterogeneous phosphorous modified alumina catalyst, the DEE content produced by the ethanol dehydration process with SO_4/TiO_2 were still relatively higher. Research conducted by [40] discovered that a heterogenous phosphorous modified alumina catalyst that was synthesized and applied to the ethanol dehydration process at low temperature resulted in a DEE level of 0% at temperatures of 200 and 250 °C.

The significant difference in the results of DEE levels was influenced by several factors. The most effective outcome of the dehydration process of ethanol was the surface area and the pore size of the heterogeneous catalyst because these two factors significantly influenced the activity and selectivity of a catalyst. It was known that alumina catalyst had larger surface area than SO_4/TiO_2 catalyst, which was 200 m^2 g^{-1} and a pore diameter of 34.76 nm [39]. While the SO_4/TiO_2 catalyst had a larger surface area compared to the phosphorous modified alumina catalyst, that was 9.85 m^2g^{-1} and pore diameter of 29.60 nm (mesopore system), while phosphorous modified alumina catalyst had a surface area of 6 m^2g^{-1} and pore diameter of 19.75 nm [40].

4. Conclusions

The sulfation process on titania catalyst could form solid acid catalyst which had Brønsted acid and Lewis acid sites, surface area with the mesoporous system effectively increase the activity and selectivity of catalyst to diethyl ether product. The highest DEE content yield was obtained at 1.72% using the TS-3-400 catalyst with a reaction temperature of 225 °C.

Author Contributions: Conceptualization, K.W.; Data curation, A.R.P.; Formal analysis, A.R.P.; Funding acquisition, K.W.; Investigation, A.R.P.; Methodology, A.R.P.; Project administration, A.R.P.; Resources, K.W.; Supervision, K.W., S.S., S.M., A.P., A.C.W. and W.D.S.; Validation, S.S., S.M., A.P. and A.C.W.; Visualization, A.R.P.; Writing—original draft, A.R.P.; Writing—review & editing, A.R.P. All authors have read and agreed to the published version of the manuscript.

Funding: This work was funded by RISET KOLABORASI INDONESIA (RKI) 2020 Number: 813/UN1/DTLIT/DIT-LIT/PT/2020.

Conflicts of Interest: The author declare no conflict of interest.

References

1. Choopun, W.; Jitkarnka, S. Catalytic activity and stability of HZSM-5 zeolite and hierarchical uniform mesoporous MSU-S ZSM-5 material during bio-ethanol dehydration. *J. Clean* **2016**, *135*, 368–378. [CrossRef]
2. Sousa, Z.; Veloso, C.; Henriques, C.; da Silva, V. Ethanol conversion into olefins andaromatics over HZSM-5 zeolite: Influence of reaction conditions and surface reaction studies. *J. Mol. Catal. A* **2016**, *422*, 266–274. [CrossRef]
3. Varisli, D.; Dogu, T.; Dogu, G. Ethylene and diethyl-ether production by dehydration reaction of ethanol over different heteropolyacid catalysts. *Chem. Eng. Sci.* **2007**, *62*, 5349–5352. [CrossRef]
4. Gucbilmez, Y.; Dogu, T.; Balci, S. Ethylene and acetalehyde production by selective oxidation of ethanol using mesoporous V-MCM-41 catalysts. *Ind. Eng. Chem. Res.* **2006**, *45*, 3496–3502. [CrossRef]
5. Pereira, C.J. New avenues in ethylene synthesis. *Science* **1999**, *285*, 670–671. [CrossRef]
6. Silitonga, A.S.; Mahlia, T.M.I.; Ong, H.C.; Riayatsyah, T.M.I.; Kusumo, F.; Ibrahim, H.; Dharma, S.; Gumilang, D. A comparative study of biodiesel production methods for Reutealistrisperma. *Energy Source Part A* **2017**, *39*, 20. [CrossRef]
7. Bailey, B.K. Perfomance of etanol as a transportations fuel. In *Handbook on Bioetanol: Production Utilization*; Wayman, C.E., Ed.; Taylor and Francis: Washington, DC, USA, 1996; pp. 37–60.
8. El-Adawy, M.; Ibrahim, A.; El-Kassaby, M.M. An experimental evaluation of using waste cooking oil biodiesel in a diesel engine. *Energy Technol.* **2013**, *1*, 726–734. [CrossRef]
9. Arcoumanis, C.; Bae, C.; Crookes, R.; Kinoshita, E. The potential of dimethyl ether (DME) as an alternative fuel for compression-ignition engines: A review. *Fuel* **2008**, *87*, 1014–1030. [CrossRef]
10. Phung, T.K.; Busca, G. Ethanol dehydration on silica-aluminas: Active sites and ethylene/diethyl ether selectivities. *Catal. Commun.* **2015**, *68*, 110–115. [CrossRef]
11. Kosaric, N.; Duvnjak, Z.; Farkas, A.; Sahm, H.; Bringer-Meyer, S.; Goebel, O.; Mayer, D. *Ethanol in Ullmann's Encyclopedia of Industrial Chemistry*, 5th ed.; Verlag-Chemie: Weinheim, Germany, 1993; Volume A9, pp. 587–653.
12. Chadwick, S.S. *Ullmann's Encyclopedia of Industrial Chemistry*, 5th ed.; A (10); Verlagsgesellschaft: Weinhem, Germany, 1987.
13. Chen, Y.; Wu, Y.; Tao, L.; Dai, B.; Yang, M.; Chen, Z.; Zhu, X. Dehydration reaction of bio-ethanol to ethylene over modified SAPO catalysts. *J. Ind. Eng. Chem.* **2010**, *16*, 717–722. [CrossRef]
14. Phung, T.K.; Lagazzo, A.; Rivero Crespo, M.Á.; Sánchez Escribano, V.; Busca, G.A. Study of commercial transition aluminas and of their catalytic activity in the dehydration of ethanol. *J. Catal.* **2014**, *311*, 102–113. [CrossRef]
15. Alharbi, W.; Brown, E.; Kozhevnikova, E.F.; Kozhevnikov, I.V. Dehydration of ethanol over heteropoly acid catalysts in the gas phase. *J. Catal.* **2014**, *319*, 174–181. [CrossRef]
16. Rahmanian, A.; Ghaziaskar, H.S. Continuous dehydration of ethanol to diethyl ether over aluminum phosphate–hydroxyapatite catalyst under sub and supercritical condition. *J. Supercrit. Fluids* **2014**, *78*, 34–41. [CrossRef]
17. Duan, C.; Zhang, X.; Zhou, R.; Hua, Y.; Zhang, L.; Chen, J. Comparative studies of ethanol to propylene over HZSM-5/SAPO-34 catalysts prepared by hydrothermal synthesis and physical mixture. *Fuel Process. Technol.* **2003**, *108*, 31–40. [CrossRef]
18. Phung, T.K.; Hernández, L.P.; Lagazzo, A.; Busca, G. Dehydration of ethanol over zeolites, silica alumina and alumina: Lewis acidity, Brønsted acidity and confinement effects. *Appl. Catal. A* **2015**, *493*, 77–89. [CrossRef]
19. Golay, S.; Kiwi-Minsker, L.; Doepper, R.; Renken, A. Influence of the catalyst acid/base properties on the catalytic ethanol dehydration under steady state and dynamic conditions. In situ surface and gas phase analysis. *Chem. Eng. Sci.* **1999**, *54*, 3593–3598. [CrossRef]
20. Zaki, T. Catalytic dehydration of ethanol using transition metal oxide catalysts. *J. Colloid Interface Sci.* **2005**, *284*, 606–613. [CrossRef] [PubMed]
21. Carlucci, C.; Degennaro, L.; Luisi, R. Titanium dioxide as a catalyst in biodiesel production. *Catalysts* **2019**, *9*, 75. [CrossRef]
22. Arata, K.; Hino, M. Preparation of superacid by metal oxides and their catalytic action. *Matter. Chem. Phys.* **1990**, *26*, 213–237. [CrossRef]
23. Gardi, J.; Ali, H.; Xiaojun, L.; Mukhtar, H.A. Synthesis of $Ti(SO_4)O$ solid acid nanocatalyst and its application for biodiesel production from used cooking oil. *Appl. Catal A-Gen.* **2016**, *527*, 81–95. [CrossRef]
24. Ropero-Vega, J.; Aldana-Pérez, A.; Gómez, R.; Niño-Gómez, M.E.; Nino-Gomez, M.E. Sulfated titania (TiO_2/SO_4^{2-}) A very active solid acid catalyst for the esterfication of free fatty acid with ethanol. *Appl. Catal.* **2010**, *379*, 24–29. [CrossRef]
25. Ahmed, I.; Khan, N.A.; Mishra, D.K.; Lee, J.S.; Hwang, J.S.; Jhung, S.H. Liquid-phase dehydration of sorbitol to isosorbide using sulfated titania as a solid acid catalyst. *Chem. Eng. Sci.* **2013**, *93*, 91–95. [CrossRef]
26. Kamsuwan, T.; Praserthdam, P.; Jongsomjit, B. Diethyl ether production during catalytic dehydration of ethanol over Ru and Pt modified H-beta zeolite catalysts. *J. Oleo Sci* **2017**, *66*, 199–207. [CrossRef]
27. Li, Y.; Guo, Y.; Liu, Y. Synthesis of high pure TiO_2 nanoparticles from $Ti(SO_4)$ in presence of EDTA as complexing agent. *China Part.* **2005**, *3*, 240–242. [CrossRef]
28. Aghilinategh, M.; Barati, M.; Hamadanian, M. Supercritical methanol for one Put biodiesel production from *chlorella vulgaris* microalgae in the presence of CaO/TiO2 nano-photocatalyst and subcritical water. *Biomass Bioenergy* **2019**, *123*, 34–40. [CrossRef]
29. Sarvari, M.H.; Sodagar, E.; Doroodmand, M.M. Nano sulfated titania as solid acid catalyst in direct synthesis of fatty acid amides. *J. Org. Chem.* **2011**, *76*, 2853–2859. [CrossRef]
30. Nagaraj, G.; Dhayal, R.A.; Albert, I.A.; Josephine, R.L. Turning the optical band gap of pure TiO_2 via photon induced method. *Optik* **2019**, *179*, 889–894.

31. Afshar, S.; Sadehvand, M.; Azad, A.; Dekamin, M.G.; Jalali-Heravi, M.; Mollahosseini, A.; Amani, M.; Tadjarodi, A. Optimization of catalytic activity of sulfated titania for efficient synthesis of isoamyl acetate by response surface methodology. *Mon. Chem.* **2015**, *146*, 1949–1957. [CrossRef]
32. Bokhimi, X.; Morales, A.; Ortiz, E.; Lopez, T.; Gómez, R.; Navarrete, J. Sulfate ion in titania polymorphs. *J. Sol-Gel Sci. Technol.* **2004**, *29*, 31–40. [CrossRef]
33. Yang, W.; Ok, Y.S.; Dou, X.; Zhang, Y.; Yang, M.; Wei, D.; Xu, P. Effectively Remediating Spiramycin from Production Wastewater through Hydrolyzing Functional Groups using Solid Superacid TiO_2/SO_4. *Environ. Res.* **2019**, *175*, 390–401. [CrossRef]
34. Patel, A.; Brahmkhatri, V.; Singh, N. Biodiesel production by esterfication of free fatty acid over sulfated zirconia. *Renew. Energy* **2013**, *51*, 227–233. [CrossRef]
35. Almeida, R.M.; Noda, L.C.; Goncalves, N.S.; Meneghetti, S.M.P.; Meneghetti, M.R. Transesterification reaction of vegetable oils, using superacid sulfated TiO_2-base catalysts. *Appl. Catal. A Gen.* **2008**, *347*, 100–105. [CrossRef]
36. Sarve, D.T.; Singh, S.K.; Ekhe, J.D. Kinetic and mechanistic study of ethanol dehydration to diethyl ether over Ni-ZSM-5 in a closed batch reactor. *React. Kinet. Mech. Catal.* **2020**, *131*, 261–281. [CrossRef]
37. Huang, D.; Zhou, H.; Lin, L. Biodiesel: An alternative to conventional fuel. *Energy Procedia* **2012**, *16*, 1874–1885. [CrossRef]
38. Scott Fogler, H. *Elements of Chemical Reaction Engineering*, 1st ed.; Prentice Hall: Hoboken, NJ, USA, 1987.
39. Widayat, A.; Rachimoellah, M. Diethyl Ether Production Process with Various Catalyst Type. *Int. J. Sci. Eng.* **2013**, *4*, 6–10. [CrossRef]
40. Limlathong, M.; Chitpong, N.; Jongsomjit, B. Influence of Phosphoric Acid Modification on Catalytic Properties of $\gamma-\chi$ Al_2O_3 Catalysts for Dehydration of Ethanol to Diethyl Ether. *Bull. Chem. React.* **2019**, *14*, 1–8. [CrossRef]